Soft Matter

Cite this: *Soft Matter*, 2012, **8**, 9886

www.rsc.org/softmatter

PAPER

Role of fluid-density correlations in hydrodynamics: a multiparticle collision dynamics simulation study

M. Belushkin,*[a] R. G. Winkler[b] and G. Foffi*[a]

Received 13th May 2012, Accepted 15th July 2012
DOI: 10.1039/c2sm26107c

Hydrodynamic interactions play a pivotal role in the dynamical behaviour of mesoscale systems such as colloidal suspensions, yet isolating their contribution from other effects remains a key challenge. Hydrodynamic correlations within a fluid are a consequence of local momentum conservation. Hence, as is commonly believed, violation of local momentum conservation should lead to non-hydrodynamic behaviour, where long-range correlations in the fluid are absent. Here, we demonstrate that generally this is a necessary but not sufficient criterion to achieve non-hydrodynamic behaviour. The motion of a massive particle leads to density modulations within the fluid. When the mechanisms underlying the relaxation processes of such modulations are removed, the dynamical behaviour of the system becomes unphysical. We show how the density relaxation mechanisms can be reintroduced in multiparticle collision dynamics (MPC) simulations, providing a consistent description of a system without hydrodynamic interactions.

I. Introduction

As is well known, the dynamics of particles suspended in a fluid is strongly affected by hydrodynamic correlations.[1,2] This is reflected in various properties, such as the collective long-time[3,4] and short-time[5,6,12] dynamical behaviour of colloids. Dilute polymer solutions are another example, where the center-of mass motion and the monomer dynamics are governed by hydrodynamic interactions.[7–11] Even single particles in a fluid are affected, because hydrodynamic self-interactions have a significant, measurable effect on the short-time dynamics.[13,14] For simple systems, and in particular for spherical colloids, theoretical results describing the hydrodynamic reaction of the fluid are readily available.[2,3,15–20] Indeed, a description of the dynamics of single particles at long times is given by the Langevin equation

$$M\frac{\mathrm{d}^2\boldsymbol{r}(t)}{\mathrm{d}t^2} = -\gamma\frac{\mathrm{d}\boldsymbol{r}(t)}{\mathrm{d}t} + \boldsymbol{\Gamma}(t). \quad (1)$$

Here, M is the mass of the particle, $\boldsymbol{r}(t)$ its time-dependent coordinate, γ the fluid's viscous friction coefficient, and $\boldsymbol{\Gamma}(t)$ the random force which obeys the fluctuation–dissipation theorem and is commonly assumed to be Gaussian white noise.[4] In order to capture the short-time dynamics, the viscous friction coefficient has to be a time-dependent quantity.[2,16,20] This approach leads to a satisfactory description of the particle motion down to time scales, where a continuum description of the solvent remains to be applicable.[2,13,14,16,18,20]

The majority of practically interesting problems, however, cannot be treated exactly in an analytical manner. Therefore, a number of computer modeling approaches have been developed. In fact, the central role of hydrodynamic correlations was first highlighted by means of computer simulations in the 1960s.[21,22]

Computer simulations provide the opportunity to unambiguously isolate the role of hydrodynamic interactions in fluids. To this end, it is useful to first perform a simulation which takes both thermal fluctuations and hydrodynamic interactions into account, and then to perform an *identical* simulation, where hydrodynamic correlations within the solvent are suppressed.

Hydrodynamic correlations arise due to local momentum conservation. Hence, the Navier–Stokes equations state a microscopic conservation law. Therefore, violation of momentum conservation should remove hydrodynamic correlations in the system. A way to achieve this goal is to randomize and decorrelate the solvent-molecule velocities.[23–25] This idea was successfully applied to polymers in solution,[24,25] where their monomers were treated as point particles.

In the present work, we demonstrate that randomization of the velocities within the solvent is a necessary but not sufficient criterion to destroy hydrodynamic correlations in colloidal systems. Highlighting the role of density modulations in the fluid associated with the motion of a large, impenetrable particle, we demonstrate that velocity randomization removes a vital relaxation mechanism which then has to be re-introduced in other ways.

We investigate this phenomenon by employing the multiparticle collision dynamics (MPC) approach, a particle-based

[a]*Institute of Theoretical Physics, Ecole Polytechnique Fédérale de Lausanne (EPFL), CH-1015 Lausanne, Switzerland. E-mail: maxim.belushkin@epfl.ch; giuseppe.foffi@epfl.ch*
[b]*Theoretical Soft-Matter and Biophysics, Institute for Advanced Simulation, Forschungszentrum Jülich, D-52425 Jülich, Germany*

mesoscale simulation technique.[23,26,27] Proposed by Malevanets and Kapral,[28,29] this coarse-grained simulation method has a *H*-theorem,[28] satisfies the fluctuation theorem,[30] and correctly describes thermal fluctuations and hydrodynamics even at very short time scales.[13,14] It is easy to implement and has been successfully used to describe the dynamics of a very broad range of soft-matter systems.[23,26,27]

II. Simulation method

The fluid is modeled in terms of N point-like particles of mass m with continuous coordinates $\boldsymbol{r}_i$ and velocities v_i, embedded in a cubic simulation box of lateral size L with periodic boundary conditions. Each of these particles represents some finite amount of solvent rather than individual solvent molecules. The simulation evolves in two steps: streaming and collision. During streaming, in the collision-time interval δt, the particles move ballistically and their coordinates are updated according to their velocities. The collision time is one of the key parameters of the simulation since it determines the mean-free path of solvent particles. The time δt is typically larger than the time step required by a molecular dynamics (MD) integrator. After streaming, the solvent particles are sorted into cubic collision cells of lateral size a which form a collision grid. Within each cell, the velocity of every particle is rotated with respect to the cell's center-of-mass velocity by a fixed angle α around a randomly oriented rotation axis. The rotation axis is the same for all particles within a single cell, but the orientation is random for every cell and collision-time step. In order to guarantee Galilean invariance, the structure of the collision grid is shifted randomly at each collision step.[31]

We choose the following normalization: the solvent particle mass $m = 1$, the thermal energy $k_BT = 1$, and collision cell size $a = 1$, *i.e.*, mass is measured in units of m, energy in units of k_BT, length in units of a, and time in units of $t_0 = \sqrt{ma^2/k_BT}$.

In our previous study,[14] we considered embedded colloids which interact with the solvent through a shifted and truncated Lennard-Jones potential. All fluid particles, which may interact with a colloid during the collision time δt do not undergo streaming. Instead, their dynamics is treated by MD with a time step $\delta t_{MD} < \delta t$. The colloid–fluid potential is given by

$$U_{cf}(r) = \begin{cases} 4\varepsilon\left(\left(\frac{R}{r}\right)^{48} - \left(\frac{R}{r}\right)^{24}\right) + 1, & r \le 2^{1/24}R, \\ 0 & r > 2^{1/24}R. \end{cases} \quad (2)$$

where $\varepsilon = k_BT$, R denotes the radius of the colloid, and r is the distance from the center of the colloid to the solvent particle. This convenient approach avoids a strong overlap between fluid particles and colloids, and corresponds to full-slip boundary conditions at the colloid–fluid interface. In the present work, we want to also consider stick-boundary conditions. Hence, we employ the bounce-back rule when calculating the interaction between the colloid and the fluid particles, whereby the velocities of the particles participating in the collision are reversed in the centre-of-mass frame.[27,32] The bounce-back rule is applied when a solvent particle reaches the surface of a colloid, at $r = R$, and no potential is applied in this case. The collisions (in other words, solvent–solute overlaps) are resolved in time with the precision of a single molecular dynamics time step.

It has been noted that such a prescription by itself leads to finite slip at the interface because of partially filled collision cells.[33,34] This slip can partially be compensated by the implementation of phantom particles in a colloid.[27] In our case, the slip effect is expected to be negligible due to the small size of the colloidal particles considered. In any case, our results are independent of slip length.

We couple an efficient cell-level thermostat[35] to the fluid to guarantee a constant local temperature during a simulation.

III. Results

A. Single-particle simulations

We consider a single colloidal particle of radius $R = 2a$ within a solvent confined in a simulation box of lateral size $L = 32a$. The solvent density is $\rho = 10/a^3$, the collision angle $\alpha = 130°$, and the collision time $\delta t = 0.05\sqrt{ma^2/k_BT}$. The density of the colloid is equal to the density of the solvent, consequently the mass of the colloid $M = 335.1m$.

In a first step, we determine the relevant time scales from measurements of the mean-squared displacement (MSD) of the colloidal particle in MPC simulations with hydrodynamic interactions. Results of MSDs are displayed in Fig. 1 (left) for

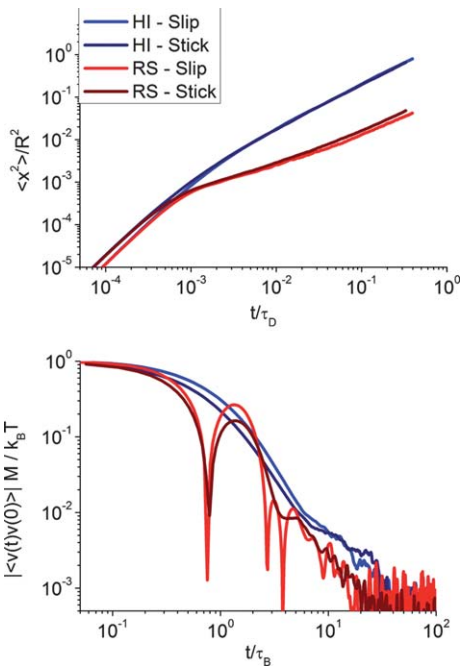

Fig. 1 Mean square displacements (top) and velocity autocorrelation functions (bottom) of the colloidal particle obtained by MPC simulations (HI) and by simulations where the velocities of the solvent particles are re-sampled from a Maxwell–Boltzmann distribution at each step (RS). Both slip and stick boundary conditions at the colloid–solvent interface are studied for both simulation protocols. For normalization, the values of τ_D and τ_B of the corresponding HI protocols are taken, for slip and stick boundary conditions, respectively.

various boundary conditions. We then obtain the following characteristic times:

• The diffusive time $\tau_D = R^2/D$, where D denotes the diffusion coefficient of the colloidal particle, is the time taken by the colloid to diffuse one radius. With the diffusion coefficients $D_{slip} = 3.16 \times 10^{-3}\sqrt{a^2 k_B T/m}$ for slip and $D_{stick} = 2.64 \times 10^{-3}\sqrt{a^2 k_B T/m}$ for stick boundary conditions, we obtain $\tau_{D,slip} = 1267\sqrt{ma^2/k_B T}$ and $\tau_{D,stick} = 1518\sqrt{ma^2/k_B T}$.

• The ballistic time $\tau_B = M/\gamma$, where $\gamma = k_B T/D$ denotes the viscous friction coefficient, is the time during which the colloid moves according to its initial momentum. With the diffusion coefficients, we find $\tau_{B,slip} = 1.06\sqrt{ma^2/k_B T}$ and $\tau_{B,stick} = 0.88\sqrt{ma^2/k_B T}$.

The classical approach to suppress HIs in MPC simulations is to randomize the velocities of the solvent particles at each step of the simulation.[23–25] This can be achieved, for example, by re-sampling the velocities from a Maxwell–Boltzmann distribution or by introducing phantom particles in the collision step.[24,25] While this approach has been shown to work for objects composed of point-like particles,[24,25] it dramatically slows down the diffusive motion of massive objects such as colloidal particles.[23] As shown in Fig. 1 (left), we confirm the slow colloid diffusion in simulations where velocities of solvent particles are re-sampled (RS) at each step, as compared to full hydrodynamic MPC simulations. This phenomenon has been interpreted in terms of Enskog friction.[23] Here, we present a different explanation.

The slow diffusion is a consequence of a caging effect. This is clearly seen from the velocity autocorrelation function (VACF) of the colloidal particle, Fig. 1 (right). Whereas the HI protocol features the standard Enskog exponential decay followed by a $t^{-3/2}$ hydrodynamic long-time tail,[14] the RS protocol generates strong anti-correlations typical of caging, rather than a simple exponential decay.

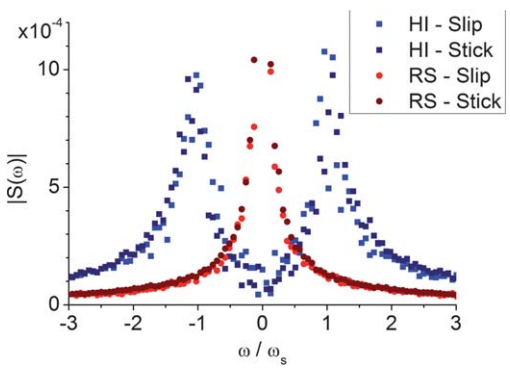

Fig. 2 Dynamic structure factors of the fluid calculated in the reference frame of the colloidal particle, for MPC simulations with hydrodynamic interactions (HI) and in simulations where the velocities of the solvent particles are re-sampled (RS) from a Maxwell–Boltzmann distribution at each step. The $\boldsymbol{k}$ vector is taken to be $2\pi/L$, with L being the lateral size of the simulation box. The solute–solvent boundary conditions have no influence on the results.

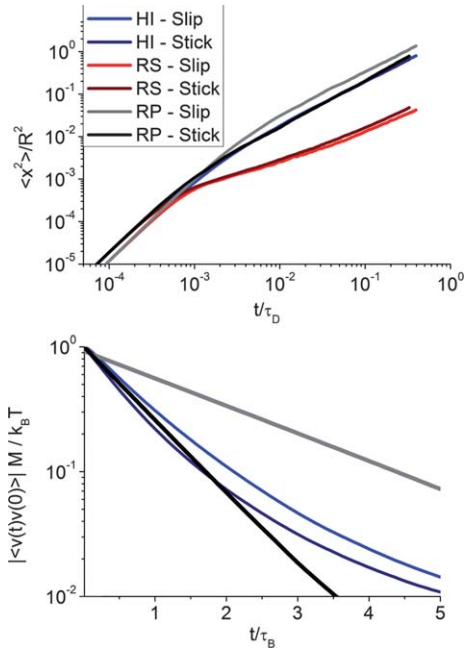

Fig. 3 Mean square displacements (top) and velocity autocorrelation functions (bottom) of a colloidal particle for MPC simulations with HIs (HI), simulations where the velocities of the solvent particles are re-sampled from a Maxwell–Boltzmann distribution at each step (RS), and simulations where, in addition to the RS protocol, positions of the solvent particles are uniformly randomized (RP). Both, slip and stick boundary conditions at the colloid–solvent interface are studied for the three simulation protocols. For normalization, the values of τ_D and τ_B of the corresponding HI protocols are taken, for slip and stick boundary conditions, respectively.

In order to understand the origin of this caging phenomenon, we consider the dynamic structure factor of the MPC fluid,[35] which we calculate in the reference frame of the colloid. The comparison of the results for both simulation protocols, displayed in Fig. 2, shows several important features:

• The results are independent of the boundary conditions at the solute–solvent interface.

• The HI protocol produces two peaks at the characteristic sound frequency $\omega_s = 2\pi v_s/L$, where $v_s = 1.0\sqrt{k_B T/m}$ denotes

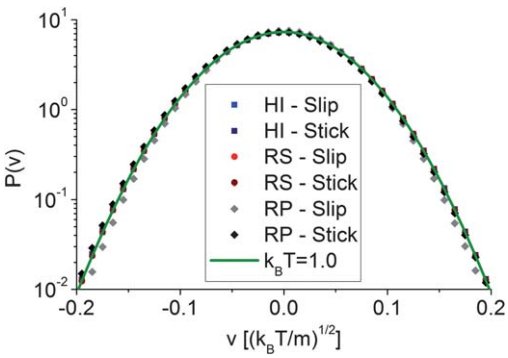

Fig. 4 Velocity distributions of a colloidal particle for various simulation protocols and solute–solvent boundary conditions. The colloid does not thermalize correctly under the RP-slip protocol, because the distribution of solvent particles within the range of the colloid's potential is not correctly reproduced.

the isothermal sound velocity. The central heat transfer peak is absent due to the thermostat.[35]

• In the RS protocol, all transport mechanisms have been removed by virtue of randomization of solvent particle velocities. Effectively, the fluid has an infinite compressibility with a zero sound velocity, and density correlations are persistent. This is indicated by a collapse of the two HI sound modes to a zero-frequency peak.

Table 1 Parameters for HI-stick and RP-stick simulations. With these parameters, we obtain diffusion coefficients for a free colloidal particle which agree within 10% accuracy for the two methods

Protocol	Box size $L[a]$	Collision time $\delta t\left[\sqrt{ma^2/k_BT}\right]$	Solvent density $\rho[m/a^3]$	Collision angle $\alpha[^\circ]$
HI-stick	60	0.02	5	90
RP-stick	60	0.1	5	90

In some sense, the RS simulation protocol features a highly non-trivial dynamics. As the colloidal particle moves through the fluid, it displaces solvent particles. Since the mechanisms responsible for the relaxation of the arising density modulations of the fluid have been removed, these modulations become persistent and lead to caging of the colloidal particle.

In order to devise a scheme for simulations without HIs, which yields a simple exponentially decaying velocity autocorrelation function of the colloidal particle, we implement the following protocol. After randomizing the velocities of the solvent particles, we additionally reposition (RP) them. The new positions are sampled from a uniform distribution, but care is taken to avoid the solute-particle's volume. In this manner, we artificially relax density modulations and restore Enskog behaviour. This is demonstrated in Fig. 3. The rate of diffusion obtained with the RP protocol is comparable to the rate of diffusion observed in HI simulations, and the velocity autocorrelation function exhibits a simple exponential decay indicative of random collisions between the solute and the solvent particles. Moreover, the dynamic

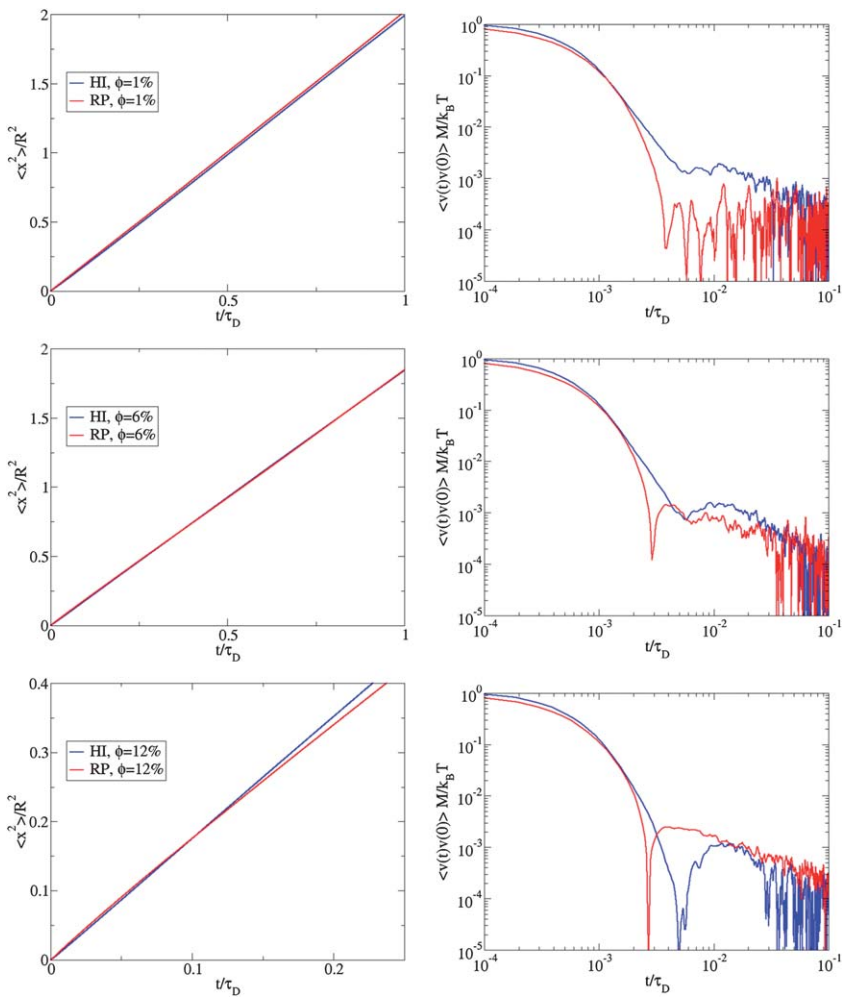

Fig. 5 Mean-square displacements and velocity autocorrelation functions of colloidal particles for the packing fractions 1% (top), 6% (middle), and 12% (bottom). The results are averaged over 10 independent runs for each packing fraction. For normalization, values of τ_D calculated for each protocol independently have been used. The simulation parameters were chosen in such a way that the diffusion coefficients – consequently τ_D, match within 10% between different protocols.

structure factor measured in simulations employing the RP protocol is zero, as desired.

The RP protocol in its present form with a random displacement of particles violates the fluid-particle-density distribution in the vicinity of solute particles, which interact with a finite-range soft potential with the fluid as, *e.g.*, for the slip boundary modelled by a Lennard-Jones potential. In the latter case, the fluid-particle-density distribution is not uniform, but determined by the Boltzmann factor. To investigate the consequent violation of the equipartition theorem, we study the probability distribution of the velocity of the colloidal particle. It is shown in Fig. 4 for the different simulation protocols. It is clearly seen that for the RP-slip protocol the equipartition theorem is violated.

B. Simulations at finite density

We have demonstrated that the RP-stick simulation protocol provides a meaningful description of a single-particle system in which hydrodynamic correlations within the fluid are absent. Here, we perform simulations at a finite colloidal packing fraction, and compare the behaviour of systems with HIs (HI-stick protocol) and without HIs (RP-stick protocol), in order to test whether correct collective behaviour appears in the RP-stick protocol.

In order to compare the two approaches, we adjust the simulation parameters in such a way that the diffusion coefficients of free colloidal particles are similar, *i.e.*, the frictional interaction with the fluid is approximately equal. Such an agreement can be achieved by adjusting the collision time step, which controls the friction and hence viscosity of the Brownian MPC solvent. The parameters for the two simulation protocols of Table 1 yield similar diffusion coefficients $D_{\mathrm{HI}} = 4.1 \times 10^{-3}\sqrt{a^2 k_{\mathrm{B}}T/m}$ and $D_{\mathrm{RP}} = 3.9 \times 10^{-3}\sqrt{a^2 k_{\mathrm{B}}T/m}$ for the HI and the RP simulation protocols, respectively. The corresponding diffusive time scales are then $\tau_{\mathrm{D,HI}} = 966\sqrt{ma^2/k_{\mathrm{B}}T}$ and $\tau_{\mathrm{D,RP}} = 1034\sqrt{ma^2/k_{\mathrm{B}}T}$. Again, the density of a colloid matches the density of the fluid, and consequently $M = 125$ m.

We perform simulations at 1%, 6%, and 12% colloid packing fractions by keeping the box size constant and changing the number of colloidal particles. All results are averaged in time and over 10 independent runs for each packing fraction. The measured mean-square displacements of colloidal particles and their velocity autocorrelation functions are presented in Fig. 5. There are a number of important points to note:

- The short-time diffusion coefficient, as given by the short-time mean squared displacement of a colloid, is essentially the same for the HI and RP simulation protocols. This emphasizes that our selected simulation parameters match the dynamical behaviour well.
- The short-time diffusion coefficient, extracted from the short-time mean squared displacement, is independent of the packing fraction, as expected.
- The velocity autocorrelation function of the RP-stick protocol decays exponentially at short times, as expected, and develops strong anti-correlations with increasing packing fraction due to colloid–colloid interactions. These are a consequence of direct colloid–colloid collisions, as no interactions are mediated by the fluid.
- The velocity autocorrelation functions of the HI-stick protocol simulations additionally show the long-time hydrodynamic tails, as expected.

Most importantly, it can be clearly seen that colloid–colloid interactions are manifested in the velocity autocorrelation functions also in the absence of hydrodynamic correlations within the fluid.

IV. Conclusions

Both, fluid-particle position and velocity correlations are important for hydrodynamic interactions. The motion of a colloid in a compressible fluid without velocity correlations leads to strong fluid-density modulations, which cause caging of the colloid and a strong slow-down of its dynamics. Hence, computer simulations, where velocity correlations are removed, do not reproduce non-hydrodynamic behaviour for a colloid. We have demonstrated that the removal of velocity correlations is a necessary but not sufficient aspect. More specifically, we find strong density modulations within the fluid associated with the motion of a massive colloidal particle in such a situation. As the transport mechanisms for density relaxation, namely directed motion of fluid particles away from the colloid, have been eliminated, entropic forces lead to the expansion of the dense fluid regions, which results in backtracking of the colloidal particle and, consequently, dramatically reduced diffusion rates.

In order to resolve this problem, we have provided a consistent prescription by repositioning the solvent particles. With this approach, we are able to perform MPC simulations with and without hydrodynamic interactions. An adjustment of the simulation parameters might be necessary to achieve the same frictional behaviour, but then MPC simulations can be performed, which differ only in the presence or lack of HIs.

We expect to observe the same solute-induced density modulations for other particle-based random-fluid simulations. Since any particle-based fluid is (more or less) compressible, solute displacements will induce local density inhomogeneities. The proposed non-hydrodynamic simulation approach is, with certain modification, also applicable to such particle-based simulation approaches. Therefore, we hope that our simulation scheme will be a valuable tool to improve the understanding of the hydrodynamic behaviour of colloidal solutions.

Acknowledgements

MB and GF acknowledge the financial support by the Swiss National Science Foundation (grant no. PP0022_119006).

References

1 G. G. Stokes, On the effect of the internal friction of fluids on the motion of pendulums, *Proc. Cambridge Philos. Soc.*, 1851, **9**, 8–106.
2 R. Zwanzig and M. Bixon, Hydrodynamic theory of the velocity correlation function, *Phys. Rev. A: At., Mol., Opt. Phys.*, 1970, **2**, 2005–2012.
3 G. K. Batchelor, Brownian diffusion of particles with hydrodynamic interaction, *J. Fluid Mech.*, 1976, **74**, 1–29.
4 J. K. G. Dhont, *An Introduction to Dynamics of Colloids; Volume 2 of Studies in Interface Science*, Elsevier, 1996.
5 P. Espanol, M. A. Rubio and I. Zuniga, Scaling of the time-dependent self-diffusion coefficient and the propagation of hydrodynamic

interactions, *Phys. Rev. E: Stat. Phys., Plasmas, Fluids, Relat. Interdiscip. Top.*, 1995, **51**, 803–806.
6 P. Espanol, On the propagation of hydrodynamic interactions, *Phys. A*, 1995, **214**, 185–206.
7 B. H. Zimm, Dynamics of polymer molecules in dilute solution: viscoelasticity, flow birefringence and dielectric loss, *J. Chem. Phys.*, 1956, **24**, 269.
8 M. Doi and S. F. Edwards, *The Theory of Polymer Dynamics*, Clarendon Press, Oxford, 1986.
9 L. Harnau, R. G. Winkler and P. Reinker, Dynamic structure factor of semiflexible macromolecules in dilute solution, *J. Chem. Phys.*, 1996, **104**, 6355.
10 R. G. Winkler, S. Keller and J. O. Rädler, Intramolecular dynamics of linear macromolecules by fluorescence correlation spectroscopy, *Phys. Rev. E: Stat., Nonlinear, Soft Matter Phys.*, 2006, **73**, 041919.
11 E. P. Petrov, T. Ohrt, R. G. Winkler and P. Schwille, Diffusion and segmental dynamics of double-stranded DNA, *Phys. Rev. Lett.*, 2006, **97**, 258101.
12 S. Henderson, S. Mitchell and P. Bartlett, Propagation of hydrodynamic interactions in colloidal suspensions, *Phys. Rev. Lett.*, 2002, **88**, 088302.
13 T. Franosch, M. Grimm, M. Belushkin, F. Mor, G. Foffi, L. Forró and S. Jeney, Resonances arising from hydrodynamic memory in Brownian motion, *Nature*, 2011, **478**, 85–88.
14 M. Belushkin, R. G. Winkler and G. Foffi, Backtracking of colloids: a multiparticle collision dynamics simulation study, *J. Phys. Chem. B*, 2011, **115**, 14263–14268.
15 E. J. Hinch, Application of the Langevin equation to fluid suspensions, *J. Fluid Mech.*, 1975, **72**, 499–511.
16 H. Metiu, D. W. Oxtoby and K. F. Freed, Hydrodynamic theory for vibrational relaxation in fluids, *Phys. Rev. A: At., Mol., Opt. Phys.*, 1977, **15**, 361–371.
17 A. N. Guz, Vibrations of a sphere in the flow of a compressible viscous-fluid, *Int. Appl. Mech.*, 1993, **29**, 959–968.
18 B. U. Felderhof, Backtracking of a sphere slowing down in a viscous compressible fluid, *J. Chem. Phys.*, 2005, **123**, 044902.
19 B. U. Felderhof, Effect of the wall on the velocity autocorrelation function and long-time tail of Brownian motion in a viscous compressible fluid, *J. Chem. Phys.*, 2005, **123**, 184903.
20 A. Erbaş, R. Podgornik and R. R. Netz, Viscous compressible hydrodynamics at planes, spheres and cylinders with finite surface slip, *Eur. Phys. J. E: Soft Matter Biol. Phys.*, 2010, **32**, 147–164.
21 B. J. Alder and T. E. Wainwright, Velocity autocorrelations for hard spheres, *Phys. Rev. Lett.*, 1967, **18**, 988–990.
22 B. J. Alder and T. E. Wainwright, Decay of the velocity autocorrelation function, *Phys. Rev. A: At., Mol., Opt. Phys.*, 1970, **1**, 18–21.
23 J. T. Padding and A. A. Louis, Hydrodynamic interactions and Brownian forces in colloidal suspensions: coarse-graining over time and length scales, *Phys. Rev. E: Stat., Nonlinear, Soft Matter Phys.*, 2006, **74**, 031402.
24 A. Malevanets and J. M. Yeomans, Dynamics of short polymer chains in solution, *Europhys. Lett.*, 2000, **52**, 231.
25 M. Ripoll, K. Mussawisade, R. G. Winkler and G. Gompper, Low-Reynolds-number hydrodynamics of complex fluids by multi-particle-collision dynamics, *Europhys. Lett.*, 2004, **68**, 106.
26 R. Kapral, Multiparticle collision dynamics: simulation of complex systems on mesoscales, *J. Adv. Chem. Phys.*, 2008, **140**, 89–146.
27 G. Gompper, T. Ihle, D. M. Kroll and R. G. Winkler, Multi-Particle Collision Dynamics – A Particle-Based Mesoscale Simulation Approach to the Hydrodynamics of Complex Fluids, *Advanced Computer Simulation Approaches for Soft Matter Sciences III*, *Adv. Polym. Sci.*, 2009, vol. 221, pp. 1–87.
28 A. Malevanets and R. Kapral, Mesoscopic model for solvent dynamics, *J. Chem. Phys.*, 1999, **110**, 8605–8613.
29 A. Malevanets and R. Kapral, Solute molecular dynamics in a mesoscale solvent, *J. Chem. Phys.*, 2000, **112**, 7260–7269.
30 M. Belushkin, R. Livi and G. Foffi, Hydrodynamics and the fluctuation theorem, *Phys. Rev. Lett.*, 2011, **106**, 210601.
31 T. Ihle and D. M. Kroll, Stochastic rotation dynamics: a Galilean-invariant mesoscopic model for fluid flow, *Phys. Rev. E: Stat., Nonlinear, Soft Matter Phys.*, 2001, **63**, 020201(R).
32 R. G. Winkler and A. Wysocki, private communication, 2010.
33 A. Wysocki, C. P. Royall, R. G. Winkler, G. Gompper, H. Tanaka, A. van Blaaderen and H. Löwen, Multi-particle collision dynamics simulations of sedimenting colloidal dispersions in confinement, *Faraday Discuss.*, 2010, **144**, 245–252.
34 J. K. Whitmer and E. Luijten, Fluid-solid boundary conditions for multiparticle collision dynamics, *J. Phys.: Condens. Matter*, 2010, **22**, 104106.
35 C.-C. Huang, A. Chatterji, G. Sutmann, G. Gompper and R. G. Winkler, Cell-level canonical sampling by velocity scaling for multiparticle collision dynamics simulations, *J. Comput. Phys.*, 2010, **229**, 168.